Structural evolution in high-pressure amorphous CO$_2$ from *ab initio* molecular dynamics

Dušan Plašienka[*] and Roman Martoňák

Department of Experimental Physics, Comenius University, Mlynská Dolina F2, 842 48 Bratislava, Slovakia

By employing *ab initio* molecular dynamics simulations at constant pressure we investigated the behavior of amorphous carbon dioxide between 0 and 100 GPa and 200 and 500 K. We focused on the evolution of the high-pressure polymeric amorphous form known as a-carbonia on its way down to zero pressure, where it eventually converts into a molecular state. During the simulations we observed a spectrum of amorphous forms between two limiting polymeric forms with different proportions of three- and four-coordinated carbon atoms. Besides that we also found a mixed molecular-polymeric form that shows pronounced metastability at certain conditions. The observed behavior suggests CO$_2$ as a possible candidate for polyamorphism. We discuss the structural and physical properties of the observed amorphous forms as well as their relation to crystalline phases.

I. INTRODUCTION

Pressure-induced amorphization (PIA) and amorphous-amorphous transition (AAT), as well as liquid-liquid transition (LLT), are fundamentally interesting and widely studied phenomena occurring in some common materials [1–3]. Especially interesting is the existence of polyamorphism, both in the solid regime AAT, as observed in H$_2$O, SiO$_2$, GeO$_2$ [4–7], Si [8], Ge [9], S [10], or C [11] and in the liquid state LLT, as reported experimentally in P [12] and S [13] (and disputed in N [14–16]) or predicted theoretically for C [17] and H [18]. Recently, carbon dioxide has been found to enrich this class of materials for observing the AAT between extended a-carbonia and molecular amorphous forms [19,20], and also for prediction of LLT between molecular and polymeric liquids [21,22].

Carbon dioxide is one of the most important compounds found on Earth and in the solar system, which plays a crucial role in planetary atmospheres and also influences the dynamics of their interiors. At the same time, the crystallography and high-pressure behavior of CO$_2$ are nontrivial and attracted a lot of attention in the last 15 years leaving some topics still unresolved (see reviews [23–25]). The exact structure of (pseudo-sixfold) phase VI (see Refs. [26–30]), intermediate character and the possible presence of bent molecules in phases II, IV, and III (see [20,31–41]), are still a matter of debate. The high-P-T regime of CO$_2$ is also disputed as far as several experiments and theoretical works often led to conflicting results [21,22,42–48]. A liquid-liquid-solid triple point was recently proposed to exist inside the Earth's geotherm region as well [21,22].

The lowest pressure solid molecular phase of CO$_2$, present on the surface of icy caps of Mars, is known as dry ice—phase I. This quadrupolar $Pa3$ structure transforms between 12 and 18 GPa into $Cmca$ phase III [31,49,50] with molecules aligned in planes, which on further compression transforms into tetrahedral phase V [31,51], recently identified as β-cristobalite $I\bar{4}2d$ structure [52,53] (though the existence of a tridymite-like $P2_12_12_1$ structure at similar conditions was also proposed [54]). Other stable phases of CO$_2$ include molecular phases II [33], IV [34,36], and VII [55]; polymeric

phase VI [26]; and other newly discovered forms—possibly polymeric phase VIII [56], two tetrahedral structures of coesite I (phase IXa) and coesite II (phase IXb) [57], and ionic phase i-CO$_2$ [47].

A specific property of phase V (and all tetrahedral structures of CO$_2$) is the extreme rigidity of the intertetrahedral C-O-C angle visible from energy calculations of the $I\bar{4}2d$ phase [58] and H$_6$C$_2$O$_7$ molecule [43], which both show a dramatic increase in energy with variation of the angle out of deep minimum placed near 125°. This behavior is in sharp contrast with SiO$_2$, where the minimum is shallow and allows silica to form a rich variety of sp^3 polymorphs [58], unlike the situation in CO$_2$. High stability of tetrahedral over possible octahedral structures in CO$_2$ is also obvious and might be connected to the small size of the carbon atoms that allows them to occupy interstitial sites of the close-packed oxygen sublattice [28]. The stiff C-O-C angle is also directly connected to the low compressibility of tetrahedral CO$_2$.

As far as the double C=O bond being one of the most stable chemical bonds, molecules sustain large overpressurization before they break and initiate transformation into a single-bonded network. Molecular phase III hence persists to (60 GPa, 300 K) and to (40 GPa, 1800 K) [31], though the equilibrium transition pressure is according to recent experiment [59] and enthalpy calculations [30,42,43] only around 20 GPa. The molecular-to-nonmolecular transition is therefore associated with high free energy barriers that lead to a negative slope of (kinetic) transition line [60] and possibly also to amorphization at low and moderate temperatures when the system is not able to complete the transition and remains stuck in a disordered state.

SiO$_2$ and GeO$_2$ are archetypal glass-forming materials exhibiting low and high density tetrahedral amorphous forms as well as octahedral forms and forms containing fivefold coordinations [4–7]. The first prediction of tetrahedra-based amorphous CO$_2$ was based on *ab initio* molecular dynamics (MD) simulations in the work of Serra *et al.* [61] in 1999 and the first observation of amorphous CO$_2$ was reported two years later [34]. It was suggested from the Raman spectra that the extended amorphous solid is formed by a mixture of three-coordinated (3c) and four-coordinated (4c) carbon atoms [34], which would be a novel property amongst the group-IV dioxides. Synthesis of a-CO$_2$ was also reported in Ref. [62] and in the further experiments, Santoro *et al.* [19]

---

*plasienka@fmph.uniba.sk

suggested from Raman spectra that the amorphous polymeric form of CO_2, named "a-carbonia," is a glassy counterpart of phase V and is also similar to tetrahedral a-silica. Another experimental study was performed at room temperature by Kume *et al.* [20] and a-carbonia was proposed to be related to phase VI. In some experiments, a-carbonia was decompressed to ambient conditions and a transformation into a molecular amorphous form was observed at 16 GPa [19] and below 30 GPa [20]. Amorphization in the higher P region occurred also on compression of phases V, VI, and coesite-CO_2 over 1 Mbar [47].

Amorphous CO_2 was studied also by first-principles simulations (MD [27] and metadynamics [29]), which confirmed the picture of the mixed three- and fourfold nature of a-carbonia. In both references a roughly equal number of 3c- and 4c-C atoms was reported. Recent *ab initio* calculations also proposed the existence of a first-order LLT between molecular and polymeric liquids [21,22]—the polymeric liquid is formed from the molecular one starting as predominantly 3c and evolves upon compression to a 4c-dominated liquid form.

The experimental and theoretical works leave several questions about amorphous carbon dioxide open. In particular, what is the actual structure of a-carbonia, what is the stable ratio of 3c and 4c carbons (3-4 ratio) at different pressures, and what is the structural relation between a-carbonia and crystalline CO_2. Furthermore, how the structural evolution from a-carbonia to the molecular amorphous form proceeds and what exactly happens upon (de)compression—if the transformations are continuous or discontinuous and whether molecules can eventually coexist with the polymeric form. In this paper, we aim at resolving these questions using *ab initio* MD.

The paper is organized as follows. In Sec. II, we describe the methods and main findings of our simulations that are analyzed in Sec. III. The analysis includes an investigation of the structural properties of polymeric amorphous forms and mixed molecular-polymeric form and their possible relation to crystalline phases. Next, the mechanical stability of the observed forms is analyzed and compared. Finally, enthalpies, compressibilities, electronic properties, and structure factors of all forms are calculated and discussed. We summarize our observations and suggestions for further study in the Conclusions.

II. SIMULATION METHODS AND PROTOCOL

We used standard density functional theory (DFT) based codes VASP 4 and 5 [63,64]. To simulate systems under constant pressure with the VASP 4 version, we employed a slightly modified Berendsen algorithm [65] where cell parameters and atomic positions and velocities were rescaled according to the difference of external and internal stress tensor every 20 MD time steps (more details are described in Ref. [66]). Simulations performed with newer versions of VASP 5 were carried out with the implemented Parrinello-Rahman (PR) barostat [67] working together with the Langevin thermostat generating the NPT ensemble. Projector augmented wave pseudopotentials and the Perdew-Burke-Ernzerhof (PBE) functional [68] were used to describe four (six) valence electrons for each carbon (oxygen) atom, using energy cutoff 450 eV and Γ-point sampling of the Brillouin zone.
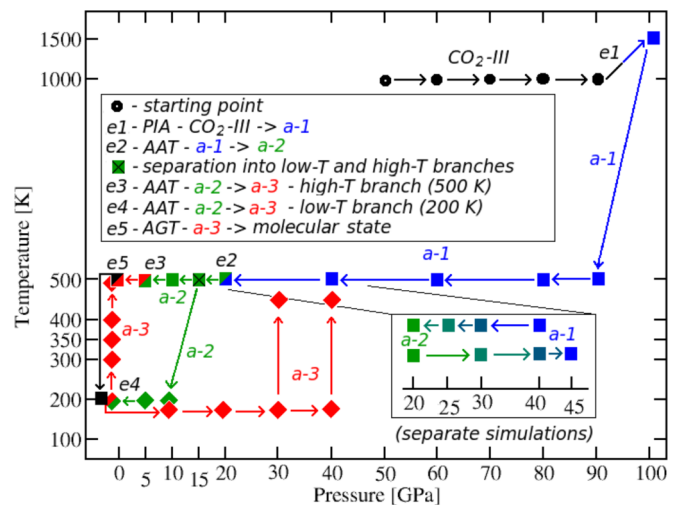

FIG. 1. (Color online) Simulation protocol of solid CO_2. Starting from phase III (black dots and arrows) at 50 GPa and 1000 K, PIA was observed at 100 GPa, event-1 (e1), leading to formation of the polymeric a-carbonia form denoted as *a-1* (blue squares and arrows). Decompression at 500 K led to the creation of another version of polymeric a-carbonia *a-2* (green squares), event-2 (e2), and on further pressure drop *a-3* (red squares) was formed at 5 GPa, event e3. The same *a-3* form (red diamonds) was created independently at 0 GPa and 200 K, e4. In the 500 K simulation branch, a molecular state (black) appeared at 0 GPa, e5. In the inset are shown separate simulations of compression of *a-2* and decompression of *a-1* between 20 and 45 GPa at 500 K performed in more pressure steps and for longer times as in the original simulation. The turquoise color of the squares represents forms with intermediate character between blue *a-1* and green *a-2*.

We ran all simulations on fairly large systems consisting of 108 CO_2 molecules. After optimization of phase III (black) to 50 GPa, we started dynamical simulations by heating the system to 1000 K and then increasing pressure in 10 GPa steps (Fig. 1). The sample amorphized upon compression from (90 GPa, 1000 K) to (100 GPa, 1500 K) similarly to previous DFT simulations [61]. The resulting polymeric a-carbonia form (blue), which we denote as *a-1* here, was dominated by 4c carbons (CO_4 tetrahedras). From this point, we started decompression at a temperature of 500 K in order to study the evolution of the amorphous state. After bringing the system to 20 GPa, *a-1* was transformed to a different polymeric form, *a-2* (green), with a similar proportion of 3c and 4c carbons. Amorphous forms *a-1* and *a-2* appear in our simulations as two limiting (high and low pressure) realizations of polymeric a-carbonia because they transform into each other gradually between 20 and 45 GPa as observed in separate calculations shown in the inset of Fig. 1.

Afterwards, we proceeded with decompression along two separate pathways - at 500 K and at 200 K [69]. In the 500 K branch we observed a formation of mixed molecular-polymeric form, *a-3* (red) at 5 GPa, while the same form appeared also in the lower 200 K branch at 0 GPa. The two independent kinetic pathways leading to the same amorphous form, with equal proportion of coordinations, suggest that the *a-3* form is not a mere artifact of the simulation time scale, but instead a form with pronounced metastability. This is further

supported by the stability of the *a-3* form obtained at 0 GPa and 200 K on its subsequent compression to 40 GPa and 500 K (see Fig. 1). In the 500 K branch, *a-3* completely depolymerized into a molecular state (black) at 0 GPa, which behaved like gas (therefore denoted as amorphous-gaseous transition—AGT in Fig. 1) and solidified to molecular amorphous form at 200 K. The total simulation time of our 324 atomic system exceeds 1 ns.

III. RESULTS AND DISCUSSION

To characterize the various amorphous forms, we analyzed the proportion of different carbon coordinations. In Fig. 2, we show the entire run of initial compression and 500 K branch decompression from Fig. 1 spanning a total simulation time of 208 ps, where all amorphous states were observed. The amount of carbon two (CO_2 molecules), three, and four coordinations are shown in red, green, and blue, respectively.

Compression from 90 to 100 GPa (starting at 52 ps) caused an immediate breakdown of all molecules and the formation of a fully extended disordered network, *a-1*, with 88% of $4c$ carbons and the remaining 12% of $3c$ atoms. The form *a-1* persisted unchanged on decompression to 40 GPa, but at 20 GPa (at 100 ps) a number of bonds desaturated and a new mixed $3c$ (40%) and $4c$ (55%) form, *a-2* containing also 5% of molecules, appeared. During simulations at 5 GPa, this form transformed into *a-3* (at about 155 ps) consisting of 18% $4c$ carbons, 60% $3c$ carbons, and 22% molecules (the same as in the lower 200 K branch). At 0 GPa and 500 K, *a-3* finally started to decay (at 185 ps) and all molecules were recovered shortly after (at 199 ps).

Separate simulations of the compression of *a-2* from 10 to 45 GPa and decompression of *a-1* from 40 to 20 GPa at 500 K

(inset of Fig. 1) revealed that both forms gradually transform into each other in this pressure window, which can be viewed as a continuous transformation between the two limiting states of polymeric a-carbonia: the high-pressure tetrahedral form *a-1* and the low-pressure form *a-2*. The forms are limiting in the sense that further compression of *a-1* does not induce further structural transformation (bonds are saturated) and decompression of *a-2* leads directly into a different amorphous regime represented by the mixed molecular-polymeric form *a-3* (and not to a different polymeric state).

A. Structure of nonmolecular a-carbonia

Amorphization occurs very fast upon the compression to 100 GPa and is accompanied by a large volume collapse and complete structural reorganization. From the distribution of intramolecular O=C=O angles, we observed that molecules always remained linear lacking any systematic bending before the onset of amorphization.

The structure of the *a-1* form is shown in Fig. 3(a), where a nanocrystallite [70] of phase V seems to be formed inside the amorphous network. This points to a structural correspondence between the tetrahedral-like form of a-carbonia, *a-1*, and crystalline phase V. To prove their relation, short-range order of both forms was investigated and depicted in Fig. 4. Radial distribution functions (RDFs; upper panel) and angular distribution functions (ADFs; lower panel) of *a-1* and phase V are shown along each other, while all distribution peaks
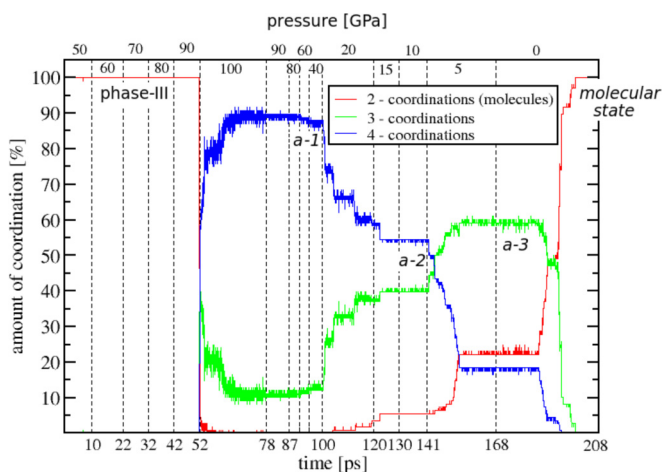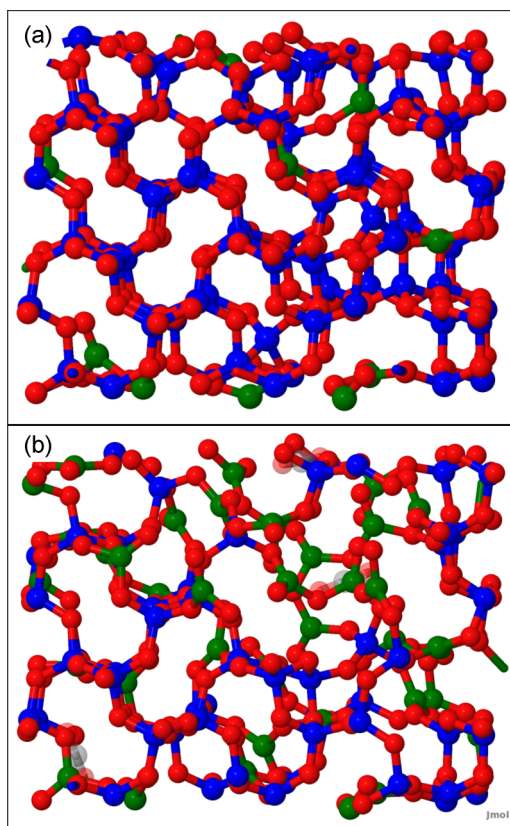

FIG. 2. (Color online) Amount of carbon coordinations (%) on compression (to 78 ps), where *a-1* was formed, and on the higher-*T* branch (500 K) decompression (from 78 to 208 ps), where all other forms appeared. The CO_2 molecules are shown in red (starting and ending at 100%), $3c$ are in green, and $4c$ in blue (the $4c$ curve is systematically larger than the $3c$ curve from 52 to 144 ps and lower thereafter). Vertical dashed lines divide the graph into regions of different simulation pressures that are labeled on the top and are changed at corresponding times labeled at the bottom. The coordination limit was 1.7 Å.

FIG. 3. (Color online) (a) Snapshot of *a-1* at 40 GPa and (b) of *a-2* at 20 GPa and 500 K. $4c$ and $3c$ carbon atoms are marked as blue and green spheres, respectively. Pictures were generated by JMOL [72].
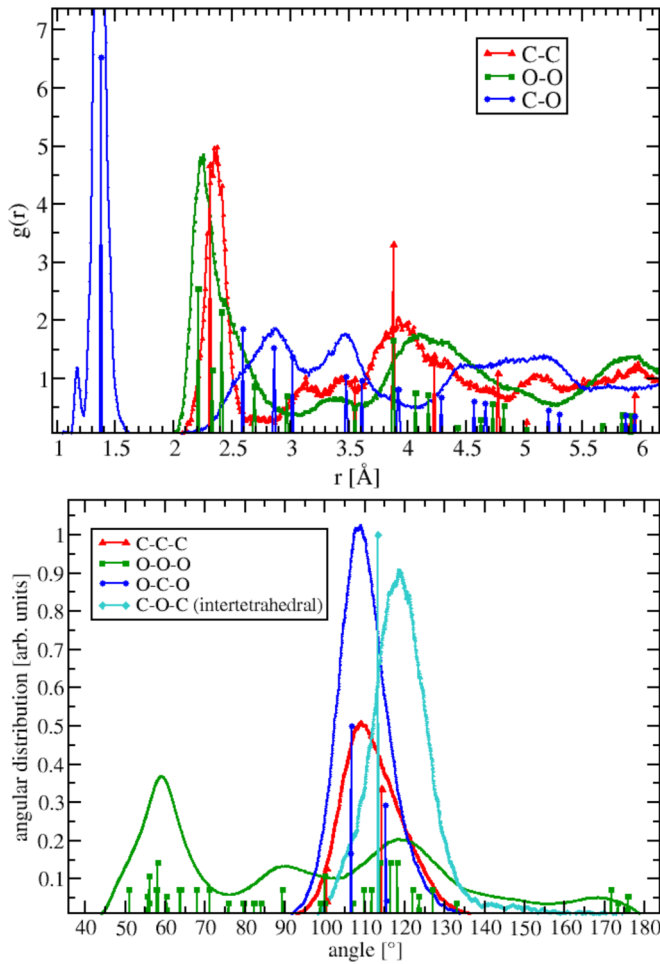
FIG. 4. (Color online) Upper panel: RDFs of type C-C (red triangles), O-O (green squares), and C-O (blue circles) for *a-1* at 40 GPa, 500 K (broad peaks) and zero-*T* structure of phase V at 41 GPa from data provided by Datchi *et al.* [52] (sharp peaks). The tiny first C-O peak represents C=O bonds from a small number of *3c* carbons. Lower panel: ADFs of type C-C-C (red triangles), O-O-O (green squares), O-C-O (blue circles), and intertetrahedral C-O-C (turquoise diamonds), all calculated within the first RDF minima of *a-1*.

of *a-1* are broad and of phase V are sharp. One can clearly see from the figures that all broad peaks of *a-1* well cover the corresponding sharp peaks of phase V. Regarding the nearest neighbors, the value of the C-C coordination number N_C^{CC} of *a-1* is 3.83 at cutoff 2.6 Å and $N_C^{OO} = 11.87$ at 2.7 Å. The C→O coordination $N_C^{C \to O} = 3.88$ and the O→C coordination $N_C^{O \to C} = 1.94$ at cutoff 1.7 Å. The corresponding coordination numbers for phase V are similar: 4, 12, 4, and 2, respectively, at the same cutoff values. The *a-1* form can therefore be regarded as an amorphous version of phase V, as was suggested for experimentally observed a-carbonia from its Raman spectra [19].

An important property of phase V is rigidity of the intertetrahedral C-O-C angle. The peak of the C-O-C ADF in *a-1* is placed around 118° (Fig. 4, lower panel, turquoise curve). This is in good agreement with the calculated ideal values (125°–130° [58] or 124° [43]) and also with the measured angle (113.2° [52]). The distribution is, however,

quite sharp for an amorphous solid (compare, e.g., with the wide Ge-O-Ge distribution in a-germania [71]) and indicates that stiffness of the C-O-C angle is a basic property of CO_2 that is inherited into the amorphous regime.

An amorphous form similar to our predominantly tetrahedral *a-1* form was reported in the previous MD simulations [61]. In the original study, it was described as a tetrahedral amorphous solid, while in the subsequent work [27], it was stated that it contained an unspecified number of unsaturated bonds (we remind one that *a-1* also contains 12% of *3c* carbons). A glass with a similar structure can be obtained by quenching from the *4c*-dominated liquid state [22].

The second limiting a-carbonia form *a-2* [Fig. 3(b)] contains only a slightly higher number of *4c* than *3c* carbons. Very similar forms like this were obtained in the previous *ab initio* simulations, which were performed along different *P-T* pathways [27,29]. Direct experimental evidence about the quantities of carbon coordinations (as determined, e.g., for amorphous GeO$_2$ [7]) is as yet not available.

B. Structure of molecular-polymeric form

At two different *P-T* points (e3 and e4 in Fig. 1), the *a-2* form independently transformed into a substantially different molecular-polymeric amorphous state *a-3*, shown in Fig. 5(a). To our knowledge this form of a-CO$_2$ was not discussed so far. The *a-3* form represents a mechanically stable local packing of CO$_2$, CO$_3$, and CO$_4$ units forming a bridge between molecular and polymeric amorphous states. The form is composed of
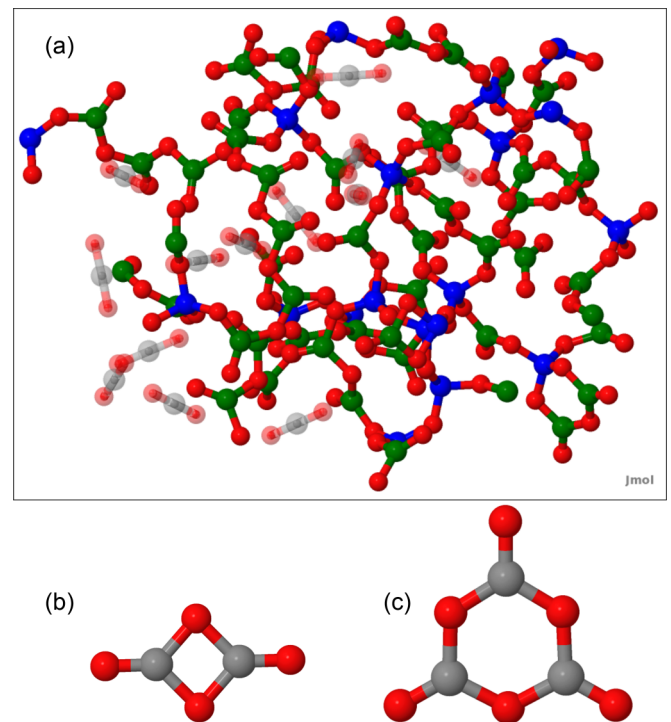

FIG. 5. (Color online) (a) Amorphous form *a-3* at 5 GPa and 500 K. One closed chain of two *3c* atoms pinned to one *4c* carbon is placed near the down right edge of the picture. *4c* and *3c* carbons are distinguished as blue and green atoms; isolated CO$_2$ molecules are marked translucent. (b) C$_2$O$_4$ dimer and (c) C$_3$O$_6$ trimer occurring in the *a-3* form.
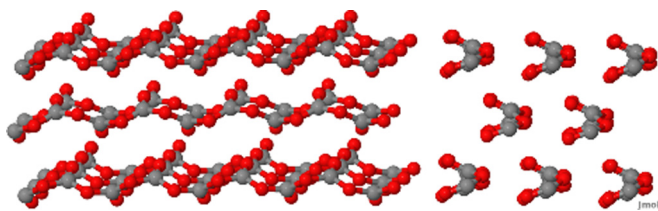
FIG. 6. (Color online) Phase *3C* at 10 GPa: front view (left) and chain axis direction side view (right).

three basic units: sp^3 tetrahedras, CO_4; triangles, CO_3; and linear molecules CO_2 [73]. The molecules remain isolated, while $3c$ and $4c$ carbons connect and form several structural patterns. The most abundant are polymeric chains formed by series of $3c$ carbons pinned to two different $4c$ carbons (nodes), which are present in various lengths and torsions. Next, we observe closed chains beginning and ending in the same $4c$ carbon and occasionally also entirely three-coordinated loops (cyclic molecules) shown in Figs. 5(b) and 5(c). Some of the cyclic $(CO_2)_x$ oligomers were already studied by methods of theoretical chemistry [74,75].

Formation of C_2O_4 dimeric molecules were observed in MD of high-*T* liquid phases [22,76]. In Ref. [76], for example, metastability of dimers, which we indeed observe in *a-3*, was proposed to take place at low temperature. Moreover, it was also suggested that the existence of these dimers may represent a kinetic intermediate step on the transformation to some three-coordinated crystalline phase, which is discussed in the next paragraph. In another theoretical study of liquid CO_2, the presence of unstable CO_2 molecules in predominantly polymeric liquid form near the proposed LLT line region [22] was also observed. This indicates that a

mechanically stable mixture of molecular and nonmolecular states at low temperatures (in solid state), where the kinetics is considerably slower, may be possible.

We now briefly discuss the possible thermodynamical background of amorphous forms containing $3c$ carbon atoms. The presence of these $3c$ carbons in a-carbonia and also in form *a-3* opens a natural question whether $3c$-C can form some stable or at least metastable structure. While no such phase has been observed experimentally, some theoretical hints exist [27,75,76]. In our case, the fact that *a-3* contains chains of $3c$-C as basic building blocks points to its possible relation to a hypothetical crystalline phase composed of infinite parallel chains. The possibility of such chain forms has been proposed in some previous studies [27,75,76]. The initial guess in our search for the $3c$ form was inspired by Ref. [27] and a picture of the structure is depicted in Fig. 4(b) therein. Performing optimizations at several pressures, we found a structure denoted as phase *3C*, which is formed by linear zigzag chains aligned in mutually shifted planes (Fig. 6). Phase *3C* has lower enthalpy than molecular phases at pressures over 40 GPa (see Fig. 8). Structural data and *d* spacing [77] of this phase can be obtained from the Supplemental Material [78]. Phase *3C* was stable in dynamical simulations at 0 GPa and 200 K for several tens of picoseconds.

C. Structural stability

We turn now to a discussion of the behavior of the observed amorphous forms upon change of pressure, namely, a gradual transformation between limiting polymeric forms *a-1* and *a-2* and pronounced metastability of the molecular-polymeric *a-3* form. To relate the stability upon compression to the network structure we analyzed the distribution of nearest distances between possible reaction sites, namely, $3c$ carbons and single-coordinated ($1c$) oxygen atoms (with double bonds).
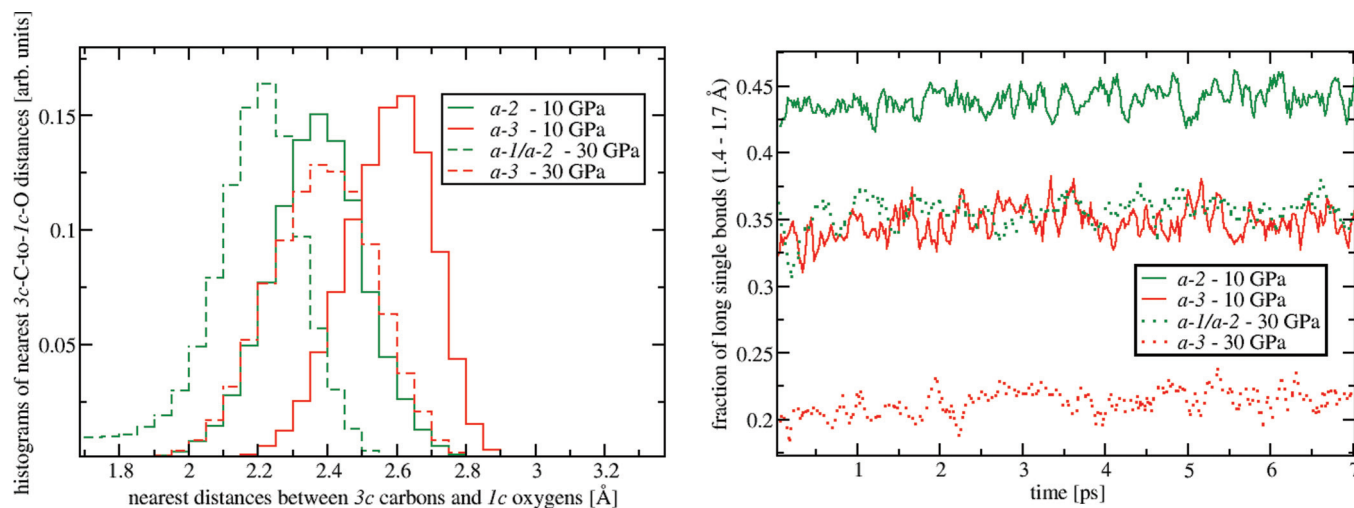

FIG. 7. (Color online) (a) Histograms of nearest distances between $3c$ carbons and $1c$ oxygens for polymeric a-carbonia *a-2* (green histogram) at 10 GPa and intermediate state *a-1/a-2* (dashed green) at 30 GPa and *a-3* at 10 GPa (red), and at 30 GPa (dashed red), all at 500 K. The histograms are scaled to the total number of $3c$ carbons in the system. (b) Fraction of C-O single bonds with length between 1.4 and 1.7 Å calculated for each frame during a 7 ps time interval extracted from the MD runs and scaled to total numbers of C-O single bonds. Colors and line styles represent the same systems and conditions as in (a); systems at 30 GPa are marked with dotted lines. Full lines and dashed/dotted lines are to be compared separately as different line styles represent different simulation pressures and line colors distinct between polymeric and *a-3* form.

The distribution of the nearest distances between $3c$-C and $1c$-O atoms reflects the potential ability to turn $3c$ carbons into $4c$ ones upon compression. The respective histograms are shown in Fig. 7(a) where we compare at 10 GPa a-3 and a-2 and at 30 GPa a-3 and an intermediate state between a-1 and a-2 (containing 63% of $4c$ carbons). At both pressures of 10 and 30 GPa, histograms of a-3 are shifted away from the corresponding polymeric ones indicating that less possible reaction sites of $3c \rightarrow 4c$ C transitions are available. Moreover, at 30 GPa, the a-1/a-2 state contains a sizable amount of nearest $3c$-C-to-$1c$-O distances between 1.7 and 2 Å, which allows for gradual evolution of coordinations in the polymeric regime between the limiting forms a-1 and a-2.

The structural stability of the system during decompression, on the other hand, can be related to the relative number of most strained single C-O bonds which are prone to break during the volume increase. To this end we count the fraction of elongated single bonds in the length interval from 1.4 to 1.7 Å [Fig. 7(b)]. It can be clearly seen that the a-3 form compared to polymeric forms contains a lower amount of elongated single bonds and thus is more stable also with respect to decompression.

D. Thermodynamical, mechanical, electronic, and structural properties

To analyze relative zero-T stability of the discussed amorphous and crystalline forms, we calculated equations of state for volume and enthalpy versus pressure [Figs. 8(a) and 8(b), respectively]. Our calculated enthalpy functions show that phase V becomes more stable than phase III over 17.5 GPa and molecular phase I crosses the phase-III curve at around 20 GPa, similarly to Ref. [39]. The three-coordinated phase $3C$ (stable up to 60 GPa) is favored over phase V below 8 GPa and over phase III above 40 GPa, though it is metastable at all pressures. Regarding the amorphous forms, the a-1 curve systematically copies the curve of its crystalline counterpart phase V with about 0.7 eV higher enthalpy. The a-2 form survived optimization only between 10 and 20 GPa, while a-1 decayed below 30 GPa. This nonstability of both limiting polymeric forms between 20 and 30 GPa observed in the optimization process is related to the existence of the pressure window, where intermediate states between a-1 and a-2 were observed in the MD simulations (see inset of Fig. 1). Form a-3 was stable between 0 and 50 GPa and its enthalpy evolves similarly as enthalpy of phase $3C$. The enthalpies show that in certain pressure intervals, the amorphous forms are more favored compared to some competing crystalline phases and might synthesize at carefully chosen experimental P-T conditions.

To calculate bulk moduli of the investigated forms, we performed simulations with the Parrinello-Rahman barostat to obtain volume fluctuations $\langle \delta V^2 \rangle$ for NPT ensemble. These fluctuations are proportional to the isothermal bulk modulus B according to the fluctuation formula [79]

$$B = \frac{kT}{V} \langle \delta V^2 \rangle_{NPT},$$

where V is average volume.

All calculated values of B (Table I) were extracted from separate MD trajectories at 200 K lasting 40–60 ps to assure converged values of $\langle \delta V^2 \rangle_{NPT}$. From the table we see that upon progressive transformation from a-1 to molecular
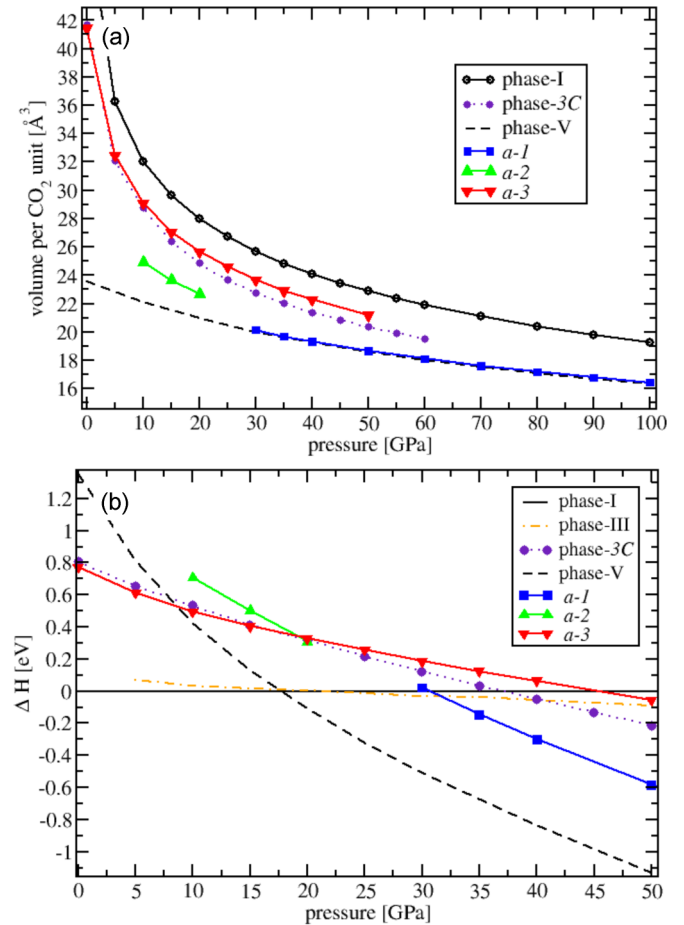

FIG. 8. (Color online) (a) Equations of state for V(P): volume per CO_2 unit versus pressure of phase I (line with empty circles), phase V (dashed line), phase-$3C$ (violet dotted line with circles) and amorphous a-1 (blue squares), a-2 (green up triangles) and a-3 (red down triangles) in 1 Mbar range. (b) Enthalpies from 0 to 50 GPa relative to phase I (horizontal line) per CO_2 unit of crystalline phase III (orange dashed-dotted line), phase $3C$ (violet dotted line with circles), phase V (black dashed line) and amorphous a-1 (blue squares), a-2 (green up triangles) and a-3 (red down triangles). All phase curves are shown only in their stability regions, where they survived optimization.

TABLE I. Calculated values of B at 200 K from hardest phase V to soft molecular phases. B of phase V at 40 GPa is reaching 300 GPa corresponding very well with theoretical predictions (Dong *et al.* [58,80]) and actual recent experimental measurements (Datchi *et al.* [52]).

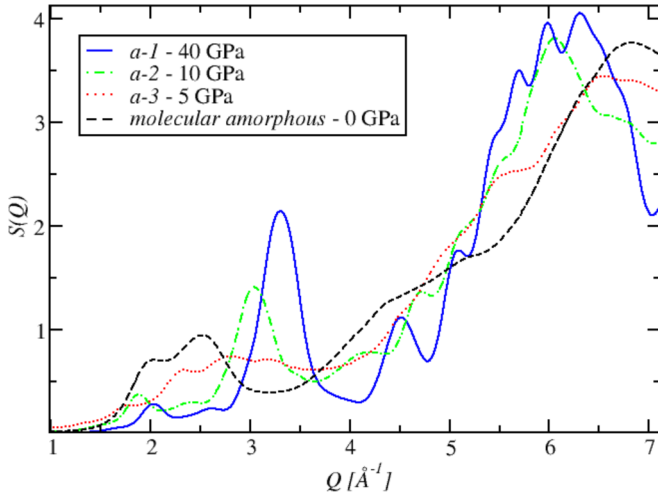| Phase	Bulk B (GPa)	P (GPa)
Phase V	294	40
a-1	282	40
a-2	75	5
a-3	46	0
Phase I	25	0
Molecular amorphous	20	0

FIG. 9. (Color online) Static structure factors of *a-1* (blue line) at 40 GPa, *a-2* (green dashed-dotted line) at 10 GPa, *a-3* (red dotted) at 5 GPa, and *molecular amorphous* form, glass (dashed black) at 0 GPa. The structural evolution from *a-1* to *a-2*, *a-3*, and to *molecular amorphous* form is represented mainly by broadening and shifting of the first main $S(Q)$ peak to lower Q, from 3.3 Å^{-1} in *a-1* to 2.5 Å^{-1} in the molecular phase.

states the value of B decreases by more than an order of magnitude. The *molecular amorphous* refers to the 200 K quenched molecular amorphous state (glass) obtained from molecular gas that appeared at the end of the 500 K branch decompression (see Fig. 1).

Next, we studied electronic properties of the amorphous forms within the PBE approximation and found that *a-3* is an insulator with an energy band gap 3.35 eV at 5 GPa and *a-2* is a semiconductor with a 1.71 eV band gap at 20 GPa. In *a-1* at 40 GPa, the gap energy is decreased to 1.48 eV, while at 90 GPa it narrows to 0.7 eV. Therefore, polymerization into a tetrahedral-like amorphous form is not followed by metallization, although closure of the band gap can be expected at Mbar conditions [24]. We remark that the predicted LLT in CO_2 is also not accompanied by metallization [22], which was noted to be exceptional for a molecular-polymeric transition in a high-T liquid state.

In order to present quantities directly comparable to experiments, we calculated static structure factors $S(Q)$ of the amorphous forms (Fig. 9). $S(Q)$ functions were calculated from the MD trajectories by the method described in Refs. [81,82]. We first calculated $S(\vec{Q}_{hkl})$ at a discrete set of $\vec{Q}_{hkl}$ vectors (determined by the periodic boundary conditions) and then made convolution with Gaussian of width 0.1 Å^{-1} to obtain $S(Q)$. This quantity was afterwards averaged over the corresponding trajectory. The normalization of the structure factors was chosen according to Ref. [19] (and the Supplemental Material therein), where $S(Q)$ was factorized to the molecular form factor $[f_C(Q) + 2f_O(Q)]^2$, where $f_C(Q)$ and $f_O(Q)$ are atomic form factors of carbon and oxygen, respectively. The calculated structure factors can then be directly compared to the experimental ones in Fig. 4 of Ref. [19]. The experimental curve at 41 GPa appears similarly to our curve of *a-1* at 40 GPa; both contain a main first peak at around 3.3 Å^{-1}. Upon decompression, our peak progressively

shifts to lower Q values, *a-2*, and becomes broader when molecules are created, *a-3*. Finally, upon transition to the molecular state (in the glass), the peak appears to become split, which is similar to the experimental data at 12 GPa, when a-carbonia was already transformed into the molecular amorphous form. This indicates that our simulated forms of a-carbonia could be associated with the earlier experimental observations [19].

IV. CONCLUSIONS

Using *ab initio* MD simulations we performed decompression of polymeric a-carbonia initially prepared at high pressure and observed several amorphous forms which behaved like mechanically stable and long-living metastable states. As the pressure decreases the original high-pressure polymeric form (*a-1*) with mostly four-coordinated carbon atoms and tetrahedral geometry first gradually transforms into less dense structures eventually reaching a limiting form (*a-2*) with a roughly equal number of four- and three-coordinated carbon atoms. Both these forms were observed in the earlier simulations [27,29,61]. Upon further decompression molecules start to appear and a new mixed molecular-polymeric form (*a-3*) is found before the system finally transforms to a fully molecular state. In the mixed form four-coordinated carbon atoms act as nodes that are connected by chains of three-coordinated carbons, while space between the chains is filled with molecules. Compared to the polymeric forms the mixed *a-3* form appears to have pronounced metastability which can be related to different distributions of certain interatomic distances and bond lengths. Due to the large gap between the time scale of experiments and simulations it is not trivial to extrapolate the metastability observed in our simulations to true metastability at experimental conditions. However, the facts that the two polymeric forms were also reported in previous simulations and that the mixed molecular-polymeric form was prepared in our simulations in two independent pathways suggest that these states might indeed represent observable amorphous phases. We believe that it would be interesting to experimentally verify our predictions by carefully monitoring the structural evolution of a-CO_2 in a slow gradual decompression performed at low temperature, where the kinetics is slower.

[1] S. M. Sharma and S. K. Sikka, Prog. Mater. Sci. **40**, 1 (1996).

[2] P. F. McMillan, J. Mater. Chem. **14**, 1506 (2004).

[3] M. C. Wilding, M. Wilson, and P. F. McMillan, Chem. Soc. Rev. **35**, 964 (2006).

[4] J. P. Itié, A. Polian, G. Calas, J. Petiau, A. Fontaine, and H. Tolentino, Phys. Rev. Lett. **63**, 398 (1989).

[5] M. Guthrie, C. A. Tulk, C. J. Benmore, J. Xu, J. L. Yarger, D. D. Klug, J. S. Tse, H-k. Mao, and R. J. Hemley, Phys. Rev. Lett. **93**, 115502 (2004).

[6] X. Hong, G. Shen, V. B. Prakapenka, M. Newville, M. L. Rivers, and S. R. Sutton, Phys. Rev. B **75**, 104201 (2007).

[7] G. Lelong, L. Cormier, G. Ferlat, V. Giordano, G. S. Henderson, A. Shukla, and G. Calas, Phys. Rev. B **85**, 134202 (2012).

[8] S. K. Deb, M. Wilding, M. Somayazulu, and P. F. McMillan, Nature (London) **414**, 528 (2001).

[9] E. Principi, A. DiCicco, F. Decremps, A. Polian, S. DePanfilis, and A. Filipponi, Phys. Rev. B **69**, 201201 (2004).

[10] C. Sanloup, E. Gregoryanz, O. Degtyareva, and M. Hanfland, Phys. Rev. Lett. **100**, 075701 (2008).

[11] Y. Lin, L. Zhang, H. K. Mao, P. Chow, Y. Xiao, M. Baldini, J. Shu, and W. L. Mao, Phys. Rev. Lett. **107**, 175504 (2011).

[12] Y. Katayama, T. Mizutani, W. Utsumi, O. Shimomura, M. Yamakata, and K. ichi Funakoshi, Nature (London) **403**, 170 (2000).

[13] R. Bellissent, L. Descotes, F. Boué, and P. Pfeuty, Phys. Rev. B **41**, 2135 (1990).

[14] G. D. Mukherjee and R. Boehler, Phys. Rev. Lett. **99**, 225701 (2007).

[15] A. F. Goncharov, J. C. Crowhurst, V. V. Struzhkin, and R. J. Hemley, Phys. Rev. Lett. **101**, 095502 (2008).

[16] B. Boates and S. A. Bonev, Phys. Rev. Lett. **102**, 015701 (2009).

[17] J. N. Glosli and F. H. Ree, Phys. Rev. Lett. **82**, 4659 (1999).

[18] S. Scandolo, Proc. Natl. Acad. Sci. USA **124**, 244704 (2006).

[19] M. Santoro, F. A. Gorelli, R. Bini, G. Ruocco, S. Scandolo, and W. A. Crichton, Nature (London) **441**, 857 (2006).

[20] T. Kume, Y. Ohya, M. Nagata, S. Sasaki, and H. Shimizu, J. Appl. Phys. **102**, 053501 (2007).

[21] B. Boates, S. Hamel, E. Schwegler, and S. A. Bonev, J. Chem. Phys. **134**, 064504 (2011).

[22] B. Boates, A. M. Teweldeberhan, and S. A. Bonev, Proc. Natl. Acad. Sci. USA **109**, 14808 (2012).

[23] M. Santoro and F. A. Gorelli, Chem. Soc. Rev. **35**, 918 (2006).

[24] C.-S. Yoo, Phys. Chem. Chem. Phys. **15**, 7949 (2013).

[25] A. R. Oganov, R. J. Hemley, R. M. Hazen, and A. P. Jones, Rev. Mineral. Geochem. **75**, 47 (2013).

[26] V. Iota, C.-S. Yoo, J.-H. Klepeis, Z. Jenei, W. Evans, and H. Cynn, Nat. Mater. **6**, 34 (2007).

[27] J. A. Montoya, R. Rousseau, M. Santoro, F. Gorelli, and S. Scandolo, Phys. Rev. Lett. **100**, 163002 (2008).

[28] M.-S. Lee, J. A. Montoya, and S. Scandolo, Phys. Rev. B **79**, 144102 (2009).

[29] J. Sun, D. D. Klug, R. Martoňák, J. A. Montoya, M.-S. Lee, S. Scandolo, and E. Tosatti, Proc. Natl. Acad. Sci. USA **106**, 6077 (2009).

[30] A. Togo, F. Oba, and I. Tanaka, Phys. Rev. B **77**, 184101 (2008).

[31] C.-S. Yoo, H. Cynn, F. Gygi, G. Galli, V. Iota, M. Nicol, S. Carlson, D. Häusermann, and C. Mailhiot, Phys. Rev. Lett. **83**, 5527 (1999).

[32] C.-S. Yoo, H. Kohlmann, H. Cynn, M. F. Nicol, V. Iota, and T. LeBihan, Phys. Rev. B **65**, 104103 (2002).

[33] V. Iota and C.-S. Yoo, Phys. Rev. Lett. **86**, 5922 (2001).

[34] C.-S. Yoo, V. Iota, and H. Cynn, Phys. Rev. Lett. **86**, 444 (2001).

[35] J.-H. Park, C. S. Yoo, V. Iota, H. Cynn, M. F. Nicol, and T. LeBihan, Phys. Rev. B **68**, 014107 (2003).

[36] F. Datchi, V. M. Giordano, P. Munsch, and A. M. Saitta, Phys. Rev. Lett. **103**, 185701 (2009).

[37] F. A. Gorelli, V. M. Giordano, P. R. Salvi, and R. Bini, Phys. Rev. Lett. **93**, 205503 (2004).

[38] B. Holm, R. Ahuja, A. Belonoshko, and B. Johansson, Phys. Rev. Lett. **85**, 1258 (2000).

[39] S. A. Bonev, F. Gygi, T. Ogitsu, and G. Galli, Phys. Rev. Lett. **91**, 065501 (2003).

[40] H. Olijnyk and A. P. Jephcoat, Phys. Rev. B **57**, 879 (1998).

[41] C.-S. Yoo, A. Sengupta, and M. Kim, High Press. Res. **31**, 68 (2011).

[42] O. Tschauner, H.-K. Mao, and R. J. Hemley, Phys. Rev. Lett. **87**, 075701 (2001).

[43] A. R. Oganov, S. Ono, Y. Ma, C. W. Glass, and A. Garcia, Earth Planet. Sci. Lett. **273**, 38 (2008).

[44] K. D. Litasov, A. F. Goncharov, and R. J. Hemley, Earth Planet. Sci. Lett. **309**, 318 (2011).

[45] Y. Seto, D. Hamane, T. Nagai, and K. Fujino, Phys. Chem. Minerals **35**, 223 (2008).

[46] N. Takafuji, K. Fujino, T. Nagai, Y. Seto, and D. Hamane, Phys. Chem. Minerals **33**, 651 (2006).

[47] C.-S. Yoo, A. Sengupta, and M. Kim, Angew. Chem., Int. Ed. **50**, 11219 (2011).

[48] A. M. Teweldeberhan, B. Boates, and S. Bonev, Earth Planet. Sci. Lett. **373**, 228 (2013).

[49] K. Aoki, H. Yamawaki, M. Sakashita, Y. Gotoh, and K. Takemura, Science **263**, 356 (1994).

[50] B. Kuchta and R. D. Etters, Phys. Rev. B **47**, 14691 (1993).

[51] V. Iota, C.-S. Yoo, and H. Cynn, Science **283**, 1510 (1999).

[52] F. Datchi, B. Mallick, A. Salamat, and S. Ninet, Phys. Rev. Lett. **108**, 125701 (2012).

[53] M. Santoro, F. A. Gorelli, R. Bini, J. Haines, O. Cambone, C. Levelutf, J. A. Montoya, and S. Scandolo, Proc. Natl. Acad. Sci. USA **109**, 5176 (2012).

[54] C.-S. Yoo, M. Kim, W. Morgenroth, and P. Liermann, Phys. Rev. B **87**, 214103 (2013).

[55] V. M. Giordano and F. Datchi, Europhys. Lett. **77**, 46002 (2007).

[56] A. Sengupta and C.-S. Yoo, Phys. Rev. B **80**, 014118 (2009).

[57] A. Sengupta and C.-S. Yoo, Phys. Rev. B **82**, 012105 (2010).

[58] J. Dong, J. K. Tomfohr, and O. F. Sankey, Phys. Rev. B **61**, 5967 (2000).

[59] A. Sengupta, M. Kim, C.-S. Yoo, and J. S. Tse, J. Phys. Chem. C **116**, 2061 (2012).

[60] M. Santoro and F. A. Gorelli, Phys. Rev. B **80**, 184109 (2009).

[61] S. Serra, C. Cavazzoni, G. L. Chiarotti, S. Scandolo, and E. Tosatti, Science **284**, 788 (1999).

[62] M. Santoro, J.-F. Lin, H.-K. Mao, and R. J. Hemley, J. Chem. Phys. **121**, 2780 (2004).

[63] G. Kresse and J. Furthmüller, Phys. Rev. B **54**, 11169 (1996).

[64] G. Kresse and J. Furthmüller, Comput. Mater. Sci. **6**, 15 (1996).

[65] H. J. C. Berendsen, J. P. M. Postma, W. F. van Gunsteren, A. DiNola, and J. R. Haak, J. Chem. Phys. **81**, 3684 (1984).

[66] D. Plašienka and R. Martoňák, Phys. Rev. B **85**, 094112 (2012).

[67] M. Parrinello and A. Rahman, Phys. Rev. Lett. **45**, 1196 (1980).

[68] J. P. Perdew, K. Burke, and M. Ernzerhof, Phys. Rev. Lett. **77**, 3865 (1996).

[69] Simulations of initial compression and 500 K branch decompression were performed with VASP 4 and Berendsen barostat, while lower-T branch decompression and all other calculations were calculated with VASP 5 and PR barostat.

[70] In the experiments, the nanocrystalline and amorphous phases also cannot always be distinguished due to the finite resolution ability of the device.

[71] J. Peralta, G. Gutiérrez, and J. Rogan, J. Phys.: Condens. Matter **20**, 145215 (2008).

[72] *Jmol: an open-source java viewer for chemical structures in 3d,* http://www.jmol.org/.

[73] C-O type RDF of *a-3* shows two distinct nearest peaks corresponding to two different C=O double bonds present in it: shorter 1.17 Å in CO_2 molecules and longer 1.18 Å coming from double bonds on $3c$ carbons.

[74] E. Lewars, Theo. Chem. **363**, 1 (1995).

[75] G. Frapper and J.-Y. Saillard, J. Am. Chem. Soc. **122**, 5367 (2000).

[76] F. Tassone, G. L. Chiarotti, R. Rousseau, S. Scandolo, and E. Tosatti, Chem. Phys. Chem. **6**, 1752 (2005).

[77] *Diamond—crystal and molecular structure visualization,* http://www.crystalimpact.com/diamond.

[78] See Supplemental Material at http://link.aps.org/supplemental/10.1103/PhysRevB.89.134105 for cif file and d-spacing pattern of phase-*3C* at 40 GPa.

[79] M. P. Allen and D. J. Tildesley, *Computer Simulation of Liquids* (Oxford University Press, New York, 1987).

[80] J. Dong, J. K. Tomfohr, O. F. Sankey, K. Leinenweber, M. Somayazulu, and P. F. McMillan, Phys. Rev. B **62**, 14685 (2000).

[81] J. M. Holender and G. J. Morgan, J. Phys.: Condens. Matter **3**, 1947 (1991).

[82] Y. Liang, Ph.D. thesis, International School for Advanced Studies (SISSA), 2007.